Molecular Vibrations of Pteridine and Two Symmetric Tetraazanaphthalenes

Jeanette K. Hurst,† Paul Wormell,‡ George B. Bacskay,† and Anthony R. Lacey*,†

School of Chemistry, University of Sydney, NSW 2006, Australia, and Centre for Biostructural and Biomolecular Research, University of Western Sydney, Hawkesbury, Richmond, NSW 2753, Australia

Received: March 30, 2000; In Final Form: May 23, 2000

The molecular vibrations of 1,4,5,8-tetraazanaphthalene (1458-TAN), 2,3,6,7-tetraazanaphthalene (2367-TAN) and pteridine are analyzed using a combination of infrared and Raman spectroscopy, ab initio calculations at the HF/6-31G* and MP2/6-31G* levels of theory, and B3LYP/4-31G and B3LYP/6-31G* density-functional calculations. New spectra are reported, and almost all of the ground-state normal modes have been identified for 1458-TAN and pteridine; the analysis for 2367-TAN is less complete. Calculated B3LYP/6-31G* vibrational frequencies provide the best correlation between theory and experiment for these compounds, but corresponding calculations using the smaller 4-31G basis are also satisfactory. The spectra of 1458-TAN and pteridine spectra exhibit a substantial number of Fermi resonances which complicate but do not prevent a detailed analysis.

I. Introduction

Nitrogen-substituted heterocycles have long attracted great spectroscopic interest: for example, the azabenzenes and azanaphthalenes have been the subject of two major reviews,[1,2] and are still actively being studied.[3,4] Indeed, new impetus has been given to this research by the development of high-level ab initio and density-functional calculations, which can make reasonably accurate predictions of electronic transition energies and vibrational frequencies in molecules of this size. Much work has been done on mono- and diaza-substituted species (i.e. molecules in which one or two C−H groups have been replaced by nitrogen atoms), but less is known about the more highly aza-substituted naphthalenes such as the tetraazanaphthalenes, which include some molecules with attractively high symmetry,[2] and offer the prospect of increasingly complex electronic spectra. We have, for example, recently analyzed the electronic spectrum of 1,4,5,8-tetraazanaphthalene (D_{2h} symmetry) using a range of experimental and computational approaches.[5] The detailed analysis of azanaphthalene and azabenzene spectra is made easier when the ground-state vibrations are well understood, particularly in the vibronic analysis of absorption and emission spectra, the analysis of hot bands and sequence structure in vapor spectra, the identification of vibronically active modes by a comparison of ground-state and calculated excited-state vibrations, and in the understanding and modeling of Duschinsky rotations in an excited electronic state.

Of the twenty-two possible tetraazanaphthalenes, three are of particular spectroscopic interest: 1,3,5,8-tetraazanaphthalene (pteridine, see Figure 1), 1,4,5,8-tetraazanaphthalene (1458-TAN) and 2,3,6,7-tetraazanaphthalene (2367-TAN). 1458-TAN and 2367-TAN retain the D_{2h} symmetry of the parent hydrocarbon, naphthalene, and thus their molecular orbitals and normal vibrational modes may be compared directly with those of naphthalene. Any perturbations may be attributed to the effects of complete aza substitution in the 1- and 2-positions, respectively. Although less symmetric, pteridine is of great intrinsic interest since it is the parent compound of a very large family of biologically important compounds.[6] It also serves as an example of a lower-symmetry tetraazanaphthalene in which symmetry reduction may introduce significant perturbations of the naphthalene orbitals and modes.

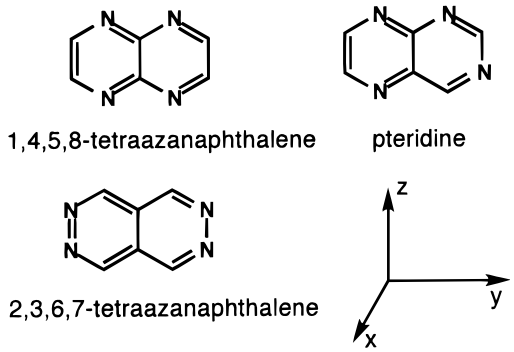

Figure 1. Axis system and molecular structures for 1,4,5,8-tetraazanaphthalene, 2,3,6,7-tetraazanaphthalene and pteridine.

In this paper we present a detailed vibrational analysis of these three compounds. New infrared and Raman spectra are correlated with ab initio and density-functional vibrational calculations, using four different levels of theory. This study aims (1) to establish which type of calculation is most suitable for modeling the molecular vibrations of this class of heterocycle, while being simple enough to be extended to three- and four-ring molecules without undue computational difficulty or cost; (2) to assign the experimental vibrational spectra of these compounds, and provide reliable predictions of vibrational frequencies that have not been detected experimentally; and (3) to establish the vibrational frequencies and normal modes for the ground-state molecules, as a basis for analyzing their electronic spectra.[5,7,8] In a related study we have studied the normal modes of several other tetraazanaphthalenes, and carried out extensive correlations of modes between molecules with different symmetries and patterns of aza substitution.[7] A subsidiary aim of the present study was to compare the normal modes of 1458-TAN, 2367-TAN, pteridine and the parent hydrocarbon, naphthalene. Bauschlicher[9] has commented that the naphthalene spectra change relatively little when C−H

* To whom all correspondence should be addressed. E-mail: a.lacey@chem.usyd.edu.au. Telephone: +61 2 9351 3105. Fax: +61 2 9351 7098.
† University of Sydney.
‡ University of Western Sydney.

10.1021/jp001222m CCC: $19.00
Published on Web 07/18/2000

groups are replaced by N during aza-substitution. Similarities between the vibrational spectra of naphthalene and the diazanaphthalenes have been used to assign the spectra of these compounds,[10,11] and Carrano and Wait[10] have published a correlation table that includes naphthalene, various azanaphthalenes and diazanaphthalenes, and also 1458-TAN. The effect on the normal modes of naphthalene of substituting four out of its eight C−H groups is briefly discussed below, and a correlation table for naphthalene and three tetraazanaphthalenes is presented. A more extensive study is reported elsewhere.[7]

1458-TAN and 2367-TAN belong to the D_{2h} point group and each molecule has a total of thirty-six normal modes, comprising seven a_g, two b_{1g}, three b_{2g}, six b_{3g}, three a_u, six b_{1u}, six b_{2u} and three b_{3u} modes. Naphthalene, which is also D_{2h}, has 12 additional modes: two a_g, one b_{1g}, one b_{2g}, two b_{3g}, one a_u, two b_{1u}, two b_{2u} and one b_{3u}. The in-plane modes are of a_g, b_{1u}, b_{2u} and b_{3g} symmetry, while the out-of-plane modes are a_u, b_{1g}, b_{2g} and b_{3u}. The b_{1u}, b_{2u} and b_{3u} modes are infrared active only; the a_g, b_{1g}, b_{2g} and b_{3g} modes are Raman active only; and the a_u modes are inactive in both types of spectrum. We have followed the axis system used by Mulliken,[12] Innes et al.[2] and Palmer,[13] as shown in Figure 1. Pteridine belongs to the C_s point group and has 25 in-plane modes of a′ symmetry and 11 out-of-plane modes of a″ symmetry. All thirty-six modes are both infrared and Raman active.

Infrared spectra of all three compounds have been reported previously, and also a Raman spectrum for 1458-TAN. These results are reviewed and, where appropriate, reassigned in the present paper. Adembri et al.[14] listed thirteen "well-resolved and sharp" infrared bands for 2367-TAN in their original report of the compound's synthesis, but no other spectral data have been reported since. Mason[15] published a spectrum for pteridine, and Armarego et al. gave a partial vibrational analysis.[16] Subsequently Armarego recorded a new spectrum for use in a study by Chappell and Ross of the out-of-plane modes of various azabenzenes and azanaphthalenes.[17] Palmer[13] reported and analyzed infrared and Raman spectra of 1458-TAN; these results were also reported by Carrano and Wait,[10] who correlated them with vibrational frequencies for naphthalene and several other azanaphthalenes. Chappell and Ross[17] have reviewed Carrano and Wait's assignments, aided by a new infrared spectrum recorded by Armarego.

The infrared frequencies for 2367-TAN have not previously been analyzed or assigned, but there have been two normal-coordinate analyses of 1458-TAN. Palmer[13] used a modified Urey−Bradley force field for in-plane modes, and a modified valence force field for out-of-plane modes, and proposed assignments for all thirty-six normal modes. Chappell and Ross[17] concentrated on the out-of-plane modes, using a transferable valence force field that they devised for the azabenzenes and azanaphthalenes, but noted that their force field may be less applicable to highly aza-substituted molecules than it is to the diazanaphthalenes. They confirmed some of Palmer's assignments, but rejected or modified others, leaving five out-of-plane modes unassigned. Since low-frequency out-of-plane modes are likely to be vibronically active in this class of compound,[18] the detailed analysis of the electronic spectrum of 1458-TAN requires more secure assignments of these modes. Chappell and Ross also proposed assignments for most of the out-of-plane modes of pteridine, but only six of the in-plane modes. Many modes remain unassigned and, again, these may be significant in the electronic spectra of the compound.

Vibrational analysis of these compounds has been transformed by the development of calculations that can use relatively large basis sets for molecules of this size, or even larger. For example, an SCF calculation at the HF/6-31G* level gives good correlation between theory and experiment for the ground-state vibrations of phthalazine (2,3-diazanaphthalene), while HF/6-31G* and MP2/6-31G* calculations have been carried out for the single-ring compound pyridazine.[3] MP2 calculations represent a higher level of theory and give a better model of electron correlation. They are significantly more expensive in computer resources, especially for molecules of lower symmetry, but do not necessarily provide as good a model of the molecular potential surface as HF or density-functional theory (DFT) calculations.[19,20] Indeed, recent studies have shown that DFT calculations using the B3LYP functional are computationally economical and give good results for naphthalene, anthracene,[20] some of their aza-derivatives,[9] and larger aromatic species.[21,22] Very good results have been obtained using the relatively small 4-31G basis set, although this involved some degree of fortuitous cancelation of errors. In the present paper we compare three different computational methods—HF, MP2 and B3LYP, all with the larger 6-31G* basis set, as well as B3LYP with the 4-31G basis—to establish which performs best with the tetraazanaphthalenes. Bauschlicher[9] found that there was good qualitative agreement between theory and experiment for compounds such as isoquinoline and quinoline; our aim has been to study this quantitatively for some more highly substituted molecules. The results have proven to be highly satisfactory.

It is important to demonstrate that molecular orbital (MO) calculations give accurate results for aza-substituted molecules of this size, since one of our aims is to extend these studies to larger molecules, including tricyclic and tetracyclic heterocycles; Bauschlicher and co-workers have similarly extended the use of DFT calculations to polycyclic hydrocarbons and their cations.[9,20,22] For these larger molecules the density of normal modes in some frequency ranges will be large,[23] and purely on statistical grounds it becomes easy to match spectral bands with theoretical predictions. This is also an issue in the current study, so the analysis of the experimental spectra has drawn on symmetry selection rules, depolarization ratios, comparisons with related molecules, solvent shifts, band intensities in the Raman and infrared spectra, as well as comparison between experimental frequencies and the various theoretical predictions.

II. Methods

Pteridine was synthesized using the method of Albert and Yamamoto[24] and purified by vacuum sublimation (mp 137−140 °C, literature 140 °C[24]). The pure compound was kept under vacuum to reduce the rate of decomposition. 2367-TAN was a gift from Prof. I. G. Ross and was used without further purification. Exhaustive attempts to repeat the only reported synthesis of 2367-TAN[14] were unsuccessful, and the amount of compound available was only sufficient for one mid-IR spectrum to be recorded.[7] Initial samples of 1458-TAN were a gift from Dr W. L. F. Armarego; additional material was prepared using his published synthesis[25] and purified by recrystallization from acetone followed by vacuum sublimation (mp >270 °C dec, literature 268 °C[25]). The pure compound was kept under vacuum to prevent decomposition.

Infrared absorption spectra of all three compounds were recorded in pressed KBr disks (400−3500 cm^{-1}) and pressed polyethylene disks (50−550 cm^{-1}) using a Bruker IFS-66V FT-infrared spectrometer. Raman spectra were recorded of solid samples of pteridine and 1458-TAN using a Bruker RFS 100 FT-Raman spectrometer with 1064 nm Nd:YAG laser excitation in a 180° backscattering arrangement. Samples were held in an

aluminum pellet, and a laser power of 50 mW was used. Polarized Raman spectra were recorded of saturated solutions of pteridine and 1458-TAN in chloroform (Merck, Uvasol, for spectroscopy). These provided depolarization ratios for the stronger bands, but some of the weaker bands could not be seen owing to the limited solubility of the compounds and their tendency to decompose when higher laser powers were used. Spectra of the neat liquids could not be recorded as the compounds started to decompose soon after melting.

Optimized ground-state molecular geometries, harmonic vibrational frequencies and infrared intensities of naphthalene and the three tetraazanaphthalenes were calculated at the Hartree−Fock SCF (HF) and second-order Møller−Plesset (MP2) levels of theory in conjunction with the 6-31G* basis, and at density-functional B3LYP/6-31G* level using the Gaussian 94 program.[26] Calculations on the tetraazanaphthalenes were also carried out at the B3LYP/4-31G level to test Bauschlicher's findings that the smaller unpolarized basis could give better results for some compounds.[9] The calculated frequencies were scaled using the following factors: 0.8929 (HF),[27] 0.9427 (MP2),[28] 0.9613 (B3LYP/6-31G*)[28] and 0.958 (B3LYP/4-31G).[20] These empirical factors partly correct for anharmonicity and deficiencies in the modeling of electron correlation, as well as limitations of the basis sets. The normal modes of the molecules were displayed graphically by exporting the Gaussian output files to the WINVIB program.[29]

III. Results and Discussion

The computed vibrational frequencies for 1458-TAN are given in Table 1, together with experimental results and the assignments of Palmer[13] and Chappell and Ross.[17] To gauge the performance of the three types of calculation using the 6-31G* basis set, we report the mean and standard deviation of the differences between experimental and scaled theoretical frequencies, together with RMS and maximum differences between theory and experiment. We have omitted any modes for which confident experimental assignments are not available but have included the high-frequency C−H stretching modes which may be appreciably anharmonic, and for which single scaling factors may not compensate adequately for this anharmonicity. These modes have been included, since this study aimed to assign bands in all regions of the spectrum. The experimental assignments for the parent compound, naphthalene, are reasonably secure and serve as a good benchmark.[30] The assignments for the azanaphthalenes have not received such sustained scrutiny, but satisfactory agreement between theory and experiment would suggest that a particular method works well for these heterocycles. Other workers have used more sophisticated scaling methods to obtain a closer fit between calculated and experimental band frequencies for aromatic molecules. For example, Bauschlicher and Langhoff found that the use of a separate scaling factor for C−H stretching modes gave more accurate B3LYP frequencies for naphthalene, except in the case of the 4-31G basis, for which very good results were obtained owing to the fortuitous cancelation of errors.[20] However, the present study aimed to use the minimum number of standard scaling factors that would give a spectroscopically useful fit between theory and experiment, and a single scaling factor was found to be satisfactory, even for the C−H modes.

Comparisons between experimental assignments[30] and our calculations for naphthalene are summarized in Table 2, together with the results for 1458-TAN, 2367-TAN and pteridine. The B3LYP/6-31G* results are superior to those at the HF/6-31G* level, although they both slightly underestimate most of the frequencies when compared with experiment. In all cases the comparisons improve when the C−H stretching modes are left out of consideration. The MP2/6-31G* results are less satisfactory, especially for the b_{2g} out-of-plane modes, which actually include one with an imaginary frequency, indicating that at the MP2 level the equilibrium geometry would be nonplanar. This result is contrary to experiment, and confirms that the MP2/6-31G* calculation does not provide a reliable potential surface for naphthalene. As noted by Bauschlicher,[20] B3LYP/4-31G calculations give very good results for naphthalene, owing to the fortuitous cancelation of various errors; they also perform well for larger molecules such as phenanthrene, chrysene and pyrene.[22]

TABLE 1: Calculated and Experimental Vibrational Frequencies for 1458-TAN

	$\bar{\nu}$/cm^{-1}						
mode	HF/ 6-31G*	MP2/ 6-31G*	B3LYP/ 6-31G*	B3LYP/ 4-31G	expt[a]	expt[b]	expt[c]
a_g modes							
ν_1	3025	3046	3062	3081	3052[d]	3058	
ν_2	1607	1504	1536	1486	1563	1577	
ν_3	1384	1369	1381	1367	1375	1376	
ν_4	1316	1307	1307	1294	1342	1247	
ν_5	1024	1037	1039	1043	1054	1055	
ν_6	753	726	746	736	763	767	767
ν_7	531	523	534	542	552	555	555
a_u modes							
ν_8	995	900	955	989		973	973
ν_9	654	620	650	668	652[f]	652	652
ν_{10}	168	131	142	146	121[f]	226	
b_{1g} modes							
ν_{11}	871	816	834	846	868	932	861
ν_{12}	425	389	409	425	408	387	411
b_{1u} modes							
ν_{13}	3008	3031	3045	3063	3052	3053	
ν_{14}	1639	1524	1582	1545	1579	1578	
ν_{15}	1383	1357	1376	1375	1389	1288	
ν_{16}	1179	1134	1162	1133	1185[e]	1117	
ν_{17}	858	859	865	877	882	869	884
ν_{18}	442	431	447	446	460	458	458
b_{2g} modes							
ν_{19}	1002	908	961	993	990	987	987
ν_{20}	833	677	817	877	823	695	
ν_{21}	479	422	464	477	469	411	
b_{2u} modes							
ν_{22}	3025	3045	3062	3080	3068[d]	3011	
ν_{23}	1490	1443	1460	1431	1474	1466	
ν_{24}	1300	1280	1287	1279	1296	1384	
ν_{25}	1115	1233	1176	1155	1174[e]	1168	
ν_{26}	931	1005	1003	1013	999	1014	
ν_{27}	561	557	570	579	588	588	590
b_{3g} modes							
ν_{28}	3008	3031	3046	3063	3067	3088	
ν_{29}	1615	1505	1543	1509	1540	1548	
ν_{30}	1475	1428	1449	1443		1346	
ν_{31}	1267	1235	1260	1265	1274	1128	
ν_{32}	945	910	930	920	954	861	932
ν_{33}	549	528	542	547	549	500	
b_{3u} modes							
ν_{34}	908	856	878	893	907	903	903
ν_{35}	530	466	503	533	508	509	509
ν_{36}	195	181	192	198	215	213	

[a] This work. [b] Reference 13. [c] Reference 17. [d] These two assignments could be exchanged. [e] These two assignments could be exchanged. [f] Tentative assignments.

1,4,5,8-Tetraazanaphthalene. In addition to the calculated frequencies for 1458-TAN, Table 1 also summarizes our experimental assignments and lists data from the earlier studies. The assignments were made using the B3LYP/6-31G* and HF/6-31G* predictions, as discussed below. The infrared and Raman

TABLE 2: Differences between Calculated and Experimental Vibrational Frequencies for Naphthalene, 1458-TAN, 2367-TAN and Pteridine

	exp frequency − calc frequency mean ± SD (RMS difference; maximum deviation)/cm^{-1}			
compound	HF/6-31G*	MP2/6-31G*	B3LYP/6-31G*	B3LYP/4-31G
naphthalene[a]	14 ± 24 (28; 69)	31 ± 42 (51; 174)	7 ± 20 (21; 73)	−4 ± 15 (16; 64)
1458-TAN	6 ± 33 (33; 75)	34 ± 32 (46; 146)	12 ± 14 (18; 37)	10 ± 26 (27; 77)
2367-TAN[b]	2 ± 31 (30; 58)		8 ± 20 (21; 40)	18 ± 34 (37; 91)
pteridine	−1 ± 28 (28; 71)		7 ± 15 (16; 37)	6 ± 27 (27; 57)

[a] Excluding b_{2g} modes. [b] Incomplete data set.

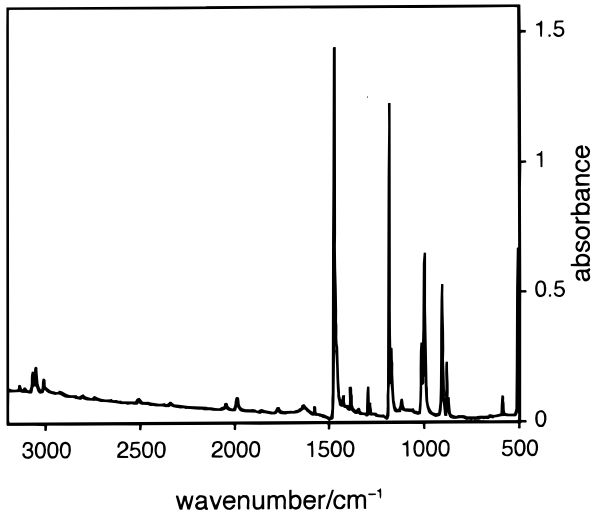

Figure 2. Infrared absorption spectrum of 1458-TAN.

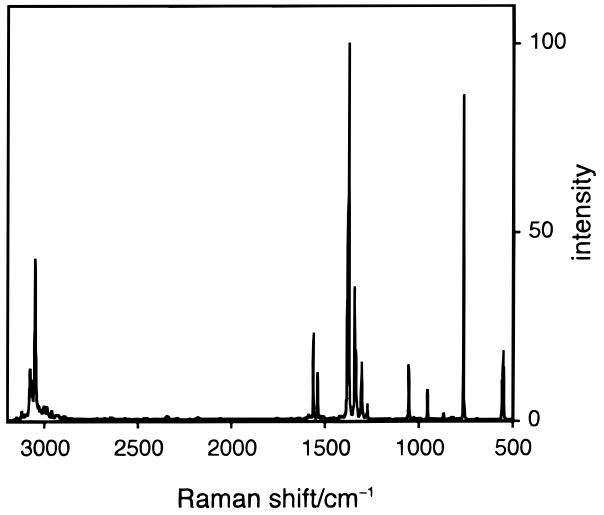

Figure 3. Raman spectrum of 1458-TAN.

spectra of 1458-TAN are shown in Figures 2 and 3, respectively, and band assignments are listed in Tables 3 and 4. Comparisons between these assignments and calculated frequencies are shown in Table 1, together with the assignments by Palmer,[13] and Chappell and Ross.[17] Relative band intensities are quoted for both spectra, together with the calculated B3LYP/6-31G* infrared intensities for the assigned modes. Vapor-phase infrared spectra could not be recorded of the compounds in this study, so we were unable to test the accuracy of the DFT intensity predictions, which apply to gas-phase molecules.

The differences between theory and experiment are shown in Table 2. The B3LYP/6-31G* and HF/6-31G* predictions led to similar band assignments, and gave similar RMS values to the naphthalene results, with the B3LYP calculation again providing the best overall fit. The results are similar to those that we have obtained for 1,8-naphthyridine (1,8-diazanaphthalene),[31] confirming that B3LYP/6-31G* calculations might profitably be extended to other related molecules. Further work is in progress on a range of monoaza- and diazanaphthalenes.[31] The MP2 calculations are again unsatisfactory, especially for the b_{2g} modes, although there are no imaginary frequencies. This may be due to the removal of steric interactions between the hydrogens on C1 and C8, and C4 and C5, respectively, which may have been responsible for the apparent out-of-plane deformation of naphthalene at the MP2 level of theory. The B3LYP/4-31G calculations are judged very satisfactory, given the smaller size of the basis set and the lower computational cost involved (the 4-31G calculations require less than half the CPU time of the 6-31G*), although better results were obtained in this case with the 6-31G* basis.

The trends in infrared band intensities correlate reasonably well with the B3LYP/6-31G* predictions, except for the C−H stretching mode ν_{22}; Bauschlicher has made similar observations.[9] Perfect correlation was not to be expected, even for very accurate DFT calculations, as the predicted intensities are for gas-phase rather than solid-state molecules, and are obtained in the double-harmonic approximation. Also, the measured relative band intensities do not allow for band overlap and Fermi resonance. However, the observed correlation, which was discovered after the spectra had been assigned largely on the basis of other criteria, supports our band assignments and indicates that calculated infrared intensities should be useful in assigning the spectra of other compounds, such as pteridine.

As mentioned above, there was good agreement between the DFT frequencies and the experimental spectra. Most of the fundamentals were easy to assign, and most of the remaining bands in the spectra can be assigned to overtones or combinations of these modes; however, several assignments require further comment. In the discussion below, predicted frequencies are B3LYP/6-31G* values unless otherwise specified.

a_g Modes. Proposed assignments: 3052, 1563, 1375, 1342, 1054, 763, and 552 cm^{-1}. Many of these assignments are reasonably secure, being based on distinct Raman bands that are polarized and agree well with predicted frequencies. The assignment of ν_7 to a frequency of 552 cm^{-1} requires comment, as the Raman spectrum has a triplet of fairly strong bands at 549, 552, and 557 cm^{-1}, but only two fundamentals and no obvious Raman-active combinations that could match them. The fundamentals are ν_7 (a_g; predicted 534 cm^{-1}) and ν_{33} (b_{3g}; predicted 542 cm^{-1}). The triplet collapses to a single band at 552 cm^{-1} in solution; this band is only partly polarized, and there may possibly be a weak shoulder near 549 cm^{-1}. The appearance and matrix dependence of the spectrum strongly suggests one or more Fermi resonances. We assign ν_7 and ν_{33} to 552 and 549 cm^{-1}, respectively, on intensity, frequency and polarization grounds, but cannot suggest an assignment for 557 cm^{-1}. This interval is not required for any combination or overtone bands in either the infrared or Raman spectra, but we

TABLE 3: Band Assignments for the Infrared Spectrum of 1458-TAN

$\bar{\nu}$/ cm^{-1}	rel intens	pred intens[a]	assignment	$\bar{\nu}$(assigned)/ cm^{-1}	$\Delta\bar{\nu}$[b]/ cm^{-1}
121	14		$\nu_{10}(a_u)$	121	
215	15	8.95	$\nu_{36}(b_{3u})$	215	
460	26	8.48	$\nu_{18}(b_{1u})$	460	
508	45	24.77	$\nu_{35}(b_{3u})$	508	
588	4.8	2.27	$\nu_{27}(b_{2u})$	588	
663	<0.2				
873[c]	4.5				
882	14	12.14	$\nu_{17}(b_{1u})$	882	
907	35	27.28	$\nu_{34}(b_{3u})$	907	
977	sh.		$\nu_{35}(b_{3u}) + \nu_{21}(b_{2g})$	508 + 469	0
999	43	33.28	$\nu_{26}(b_{2u})$	999	
1015	19		$\nu_7(a_g) + \nu_{18}(b_{1u})$	552 + 460	3
1120	3.1				
1174	17	0.03	$\nu_{25}(b_{2u})$	1174	
1185	85	45.16	$\nu_{16}(b_{1u})$	1185	
1285	2.9		$\nu_{20}(b_{2g}) + \nu_{18}(b_{1u})$	823 + 460	2
1296	6.7	0.09	$\nu_{24}(b_{2u})$	1296	
1350	0.86		$\nu_6(a_g) + \nu_{27}(b_{2u})$	763 + 588	−1
			$\nu_{17}(b_{1u}) + \nu_{21}(b_{2g})$	882 + 469	−1
1389	5.8	0.08	$\nu_{15}(b_{1u})$	1389	
1426	2.7		$\nu_{17}(b_{1u}) + \nu_7(a_g)$	882 + 552	−8
			$2\nu_{36} + \nu_{27} + \nu_{12}$	2 × 215 + 588 + 408	0
			873 + $\nu_7(a_g)$[c]	873 + 552	1
1474	100	65.69	$\nu_{23}(b_{2u})$	1474	
1579	1.8	0.37	$\nu_{14}(b_{1u})$	1579	
1638	2.0		$\nu_5(a_g) + \nu_{27}(b_{2u})$	1054 + 588	−4
			873 + $\nu_6(a_g)$[c]	873 + 763	2
1771	1.2		$\nu_{34}(b_{3u}) + \nu_{11}(b_{1g})$	907 + 868	−4
1835	<0.2		$\nu_3(a_g) + \nu_{18}(b_{1u})$	1375 + 460	0
1858	0.3		$\nu_{15}(b_{1u}) + \nu_{21}(b_{2g})$	1389 + 469	0
1902	0.3		$\nu_{19}(b_{2g}) + \nu_{34}(b_{3u})$	990 + 907	5
1925	0.7		$\nu_{34}(b_{3u}) + 2\nu_{35}(b_{3u})$	907 + 2 × 508	2
			$\nu_5(a_g)$ + 873[c]	1054 + 873	−2
1948	<0.2		$\nu_{16}(b_{1u}) + \nu_6(a_g)$	1185 + 763	0
1988	3.3		$\nu_{17}(b_{1u}) + 2\nu_7(a_g)$	882 + 2 × 552	2
			$\nu_{25}(b_{2u}) + 2\nu_{12}(b_{1g})$	1174 + 2 × 408	−2
2046	1.5		$\nu_{29}(b_{3g}) + \nu_{35}(b_{3u})$	1540 + 508	−2
			$\nu_{14}(b_{1u}) + \nu_{21}(b_{2g})$	1579 + 469	−2
2063	0.4		$\nu_{24}(b_{2u}) + \nu_6(a_g)$	1296 + 763	4
2342	0.6		$\nu_{14}(b_{1u}) + \nu_6(a_g)$	1579 + 763	0
			$\nu_{15}(b_{1u}) + \nu_{32}(b_{3g})$	1389 + 954	−1
			$\nu_{23}(b_{2u}) + \nu_{11}(b_{1g})$	1474 + 868	0
2377	0.2		$\nu_{15}(b_{1u}) + \nu_{19}(b_{2g})$	1389 + 990	−2
			$\nu_3(a_g) + \nu_{26}(b_{2u})$	1375 + 999	3
2455	<0.2		$\nu_{16} + \nu_{11} + \nu_{12}$	1185 + 868 + 408	−6
2473	<0.2		$\nu_2(a_g) + \nu_{34}(b_{3u})$	1563 + 907	3
2510	1.0		$\nu_4(a_g) + \nu_{25}(b_{2u})$	1342 + 1174	−6
2546	<0.2		$\nu_3(a_g) + \nu_{25}(b_{2u})$	1375 + 1174	−3
2657	0.3		$\nu_{15} + \nu_{11} + \nu_{12}$	1389 + 868 + 408	−8
2725	sh		$\nu_{29}(b_{3g}) + \nu_{16}(b_{1u})$	1540 + 1185	0
2741	0.5		$\nu_2(a_g) + \nu_{25}(b_{2u})$	1563 + 1174	4
2774	<0.2				
2803	0.7				
2847	0.3		$\nu_{23}(b_{2u}) + \nu_3(a_g)$	1474 + 1375	−2
2924	0.4		$\nu_{29}(b_{3g}) + \nu_{15}(b_{1u})$	1540 + 1389	−5
2946	<0.2		$\nu_2(a_g) + \nu_{15}(b_{1u})$	1563 + 1389	−6
			$\nu_{14}(b_{1u}) + \nu_3(a_g)$	1579 + 1375	−8
3000	sh		$\nu_{23}(b_{2u}) + 2\nu_6(a_g)$	1474 + 2 × 763	0
3011	3.3		$\nu_{29}(b_{3g}) + \nu_{23}(b_{2u})$	1540 + 1474	−3
3052	6.4	11.00	$\nu_{13}(b_{1u})$	3052	
3068	5.2	83.64	$\nu_{22}(b_{2u})$	3068	
3111	0.7		$\nu_{14}(b_{1u}) + \nu_{29}(b_{3g})$	1579 + 1540	−8
			$\nu_{14}(b_{1u}) + 2\nu_6(a_g)$	1579 + 2 × 763	6
3138	1.3		$\nu_{14}(b_{1u}) + \nu_2(a_g)$	1579 + 1563	−4

[a] B3LYP/6-31G* predictions (this work) in units of km mol^{-1}. [b] $\Delta\bar{\nu}$ = $\bar{\nu}$(infrared) − $\bar{\nu}$(assigned). [c] Bands for which ν_{17} = 873 cm^{-1} gives a better fit.

cannot make a convincing case for a Fermi resonance that might produce it in the crystal Raman spectrum.

The 1250−1450 cm^{-1} region of the Raman spectrum contains several strong polarized bands, but only two a_g fundamentals are expected to lie within this range: ν_3 (predicted 1381 cm^{-1}) and ν_4 (predicted 1307 cm^{-1}); the next predicted a_g mode is at 1536 cm^{-1}. The very strong, polarized doublet at 1374/1381 cm^{-1} is presumably caused by Fermi resonance involving ν_3; an excellent case can be made for this, based on intensity, polarization and calculated frequency. It is, however, hard to find a convincing assignment for the other component of the Fermi resonance. The doublet was not resolved in Palmer's spectrum,[13] and appears as a singlet in the solution spectrum, probably due to a loss of the Fermi resonance owing to different solvent shifts for ν_3 and the resonant combination or overtone. The intensity and polarization of the strong 1335/1343 cm^{-1} doublet suggest that it could be assigned to ν_4 (a_g; unperturbed frequency about 1342 cm^{-1}) in resonance with the $\nu_{17} + \nu_{18}$ combination (a_g; 1342 cm^{-1}). However, there is a significant difference (about 35 cm^{-1}) between the calculated and assigned frequencies. There is a better fit between theory and experiment for the 1304 cm^{-1} band, which is weaker but polarized (the band polarization rules out an assignment to ν_{31}, which is of b_{3g} symmetry.) However, this would leave one of the most intense features in the Raman spectrum unassigned. On the other hand, the 1304 cm^{-1} band is quite strong, and is hard to assign if ν_4 is allocated to the 1335/1343 cm^{-1} doublet. An a_g combination or overtone is required by the band polarization, but the nearest possibilities would be at 1315 cm^{-1} ($\nu_6 + \nu_7$) or, just possibly, $2\nu_9(a_u)$ where this mode would have to have a frequency of about 652 cm^{-1} (predicted 650 cm^{-1}).

In the higher-frequency region of the spectrum, the strong, polarized band at 3052 cm^{-1} is assigned to the $\nu_1(a_g$; predicted 3062 cm^{-1}) fundamental, rather than ν_{28} (b_{3g}; predicted 3046 cm^{-1}) on the basis of band intensity and polarization.

TABLE 4: Band Assignments for the Raman Spectrum of 1458-TAN

$\bar{\nu}$/ cm^{-1}	pol/depol[b]	rel intens	assignment	$\bar{\nu}$(assigned)/ cm^{-1}	$\Delta\bar{\nu}$[a]/ cm^{-1}
408	d	31	$\nu_{12}(b_{1g})$	408	
469	−	0.8	$\nu_{21}(b_{2g})$	469	
549	d?	15	$\nu_{33}(b_{3g})$	549	
552	p	19	$\nu_7(a_g)$	552	
557	−	15	Fermi?		
763	−	77	$\nu_6(a_g)$	763	
820	−	0.8	$2\nu_{12}(b_{1g})$	2 × 408	4
823	−	0.8	$\nu_{20}(b_{2g})$	823	
840	−	0.8	$2\nu_{36}(b_{3u})+\nu_{12}(b_{1g})$	2 × 215 + 408	2
868	−	4.0	$\nu_{11}(b_{1g})$	868	
954	d	7.7	$\nu_{32}(b_{3g})$	954	
990	−	0.8	$\nu_{19}(b_{2g})$	990	
1026	−	0.8	$\nu_7(a_g) + \nu_{21}(b_{2g})$	552 + 469	5
1054	p	15	$\nu_5(a_g)$	1054	
1160	−	0.8			
1274	−	2.0	$\nu_{31}(b_{3g})$	1274	
1304	p	15	$2\nu_9(a_u)$?		
1335	p	15	$\nu_4(a_g)...(\nu_{17} + \nu_{18})$	882 + 460	−7
1343	p	39	$\nu_4(a_g)...(\nu_{17} + \nu_{18})$	1342	1
1374	p	100	$\nu_3(a_g)$...Fermi	1375	−1
1381	−	46	$\nu_3(a_g)$...Fermi		
1415	−	0.8	$\nu_{34}(b_{3u}) + \nu_{35}(b_{3u})$	907 + 508	0
1520	−	0.8	$\nu_5(a_g) + \nu_{21}(b_{2g})$	1054 + 469	−3
1540	−	15	$\nu_{29}(b_{3g})$	1540	
1563	p?	23	$\nu_2(a_g)$	1563	
2948	−	0.8	$2\nu_{23}(b_{2u})$	2 × 1474	0
3052	p	38	$\nu_1(a_g)$	3052	
3067	−	7.7	$\nu_{28}(b_{3g})$	3067	
3078	−	15	$2\nu_{29}(b_{3g})$	2 × 1540	−2
3103	−	0.8	$\nu_2(a_g) + \nu_{29}(b_{3g})$	1563 + 1540	0
3122	−	2.3	$2\nu_2(a_g)$	2 × 1563	−4
3153	−	0.8	$2\nu_{14}(b_{1u})$	2 × 1579	−5

[a] $\Delta\bar{\nu}$ = $\bar{\nu}$(Raman) − $\bar{\nu}$(assigned). [b] Polarization measurements obtained in saturated chloroform solution. − denotes that a band was not seen in the solution spectrum, or was obscured by solvent bands.

a_u Modes. These are symmetry forbidden for both Raman and infrared spectra, but crystal-induced perturbations could possibly make them weakly observable. They may also contribute to overtones or combinations, but any such assignments should be treated with caution. Palmer[13] proposed assignments of 973, 652, and 226 cm^{-1}, based on normal-coordinate calculations, as well as comparisons with similar modes for related compounds, and weak features in the infrared spectrum. Chappell and Ross[17] accepted the first two assignments and discarded the third. Our infrared spectrum shows no band at 973 cm^{-1}, and the strong band at 954 cm^{-1} in the Raman spectrum is assigned to a b_{3g} mode. There is a shoulder at about 977 cm^{-1}, which is consistent with our prediction of 955 cm^{-1}, but an equally convincing assignment is $\nu_{35}(b_{3u}) + \nu_{21}(b_{2g})$. Accordingly, we cannot assign an experimental frequency to ν_8. Palmer assigned ν_9 on the basis of a weak infrared band at 652 cm^{-1}. This band is not seen in our spectrum, but there is a very weak but distinct band at about 663 cm^{-1}, which cannot convincingly be assigned to any combination band. One alternative would be to assign this band tentatively to ν_9. However, an assignment to about 652 cm^{-1} would allow the strong, polarized Raman band at 1304 cm^{-1} to be assigned to $2\nu_9$, although the source of its intensity would be questionable. Another possibility is a frequency of 687 cm^{-1} for ν_9, which would allow $2\nu_9$ to participate in a Fermi resonance with $\nu_3(a_g)$. Overall we tentatively propose that ν_9 has a frequency of about 652 cm^{-1}. Palmer assigned ν_{10} to a shoulder at 226 cm^{-1} on the higher-energy edge of the b_{3u} fundamental at 215 cm^{-1} in the infrared, rejecting an alternative assignment to an infrared band at 168 cm^{-1}, recorded in a Nujol mull. Our spectrum does not show this shoulder. The mode could be tentatively assigned to an infrared band at about 121 cm^{-1} (predicted 142 cm^{-1}), recorded in polyethylene but this is by no means secure. In summary, we tentatively assign ν_9 and ν_{10} to frequencies of approximately 652 and 121 cm^{-1}. There is no experimental assignment for ν_8, which theory suggests should lie around 950 cm^{-1}.

b_{1g} Modes. There are two modes, predicted to occur at 834 and 409 cm^{-1}. The latter, ν_{12}, correlates well with a distinct Raman band at 408 cm^{-1} and its assignment is secure. The other mode, ν_{11}, could correlate with either a very weak Raman band at 840 cm^{-1} or a stronger band at 868 cm^{-1}. Possible combination bands in this region are $2\nu_{36}(b_{3u}) + \nu_{12}(b_{1g})$ (b_{1g}; 838 cm^{-1}) and $\nu_{12}(b_{1g}) + \nu_{18}(b_{1u})$ (a_u; 868 cm^{-1}). On intensity grounds we propose that 868 cm^{-1} is $\nu_{11}(b_{1g})$, although the frequency is higher than theory suggests. An assignment of this band to the crystal-induced a_u combination is unlikely.

b_{1u} Modes. Proposed assignments: 3052, 1579, 1389, 1185, 882, and 460 cm^{-1}. The 1579, 1389, and 460 cm^{-1} assignments are reasonably secure, being based on distinct infrared bands that agree well with predicted frequencies. The high-frequency ν_{13} mode, predicted to occur at 3046 cm^{-1}, could possibly be interchanged with the $\nu_{22}(b_{2u})$ mode (predicted 3062 cm^{-1}) which is currently assigned to an infrared band at 3068 cm^{-1}. The scaled B3LYP/6-31G* calculations predict C−H stretching frequencies of the right magnitude (about 3000 cm^{-1}), with no evidence for substantial anharmonicity, but band assignments in this range will remain tentative until more accurate frequency calculations, resolved vapor spectra or accurate predictions of solid-state band intensities are available.

ν_{16} (predicted 1162 cm^{-1}) and $\nu_{25}(b_{2u})$ (predicted 1176 cm^{-1}) should also lie close to each other. There is an infrared band at 1174 cm^{-1} and a stronger band at 1185 cm^{-1}. We assign these bands to ν_{25} and ν_{16}, respectively, on the basis of the B3LYP/6-31G* predicted intensity ratios; the assignments could plausibly be exchanged. ν_{17} (predicted 865 cm^{-1}) and ν_{34} (b_{3u}; predicted 878 cm^{-1}) should also be close to each other. There are three infrared bands at 873, 882, and 907 cm^{-1} in order of increasing intensity, with 907 cm^{-1} being one of the strongest bands in the spectrum, and presumably a fundamental. On intensity grounds we assign 907 cm^{-1} to $\nu_{34}(b_{3u})$ and 882 cm^{-1} to $\nu_{17}(b_{1u})$, but cannot suggest a convincing assignment for 873 cm^{-1}. The 873 cm^{-1} frequency is not needed in the Raman spectrum, but 882 cm^{-1} is important in the strong 1335/1343 cm^{-1} Raman doublet, which is assigned as a Fermi resonance between $\nu_4(a_g)$ and $\nu_{17}(b_{1u}) + \nu_{18}(b_{1u})$ (1342 cm^{-1}). However, it is very difficult to assign all of the infrared combination bands without using the 873 cm^{-1} interval.

b_{2g} Modes. These three modes, ν_{19}, ν_{20} and ν_{21}, correlate with weak Raman bands at 990 cm^{-1} (predicted 961 cm^{-1}), 823 cm^{-1} (predicted 817 cm^{-1}) and 469 cm^{-1} (predicted 464 cm^{-1}). The first and last of these assignments are reasonably secure; the second could also be assigned to another weak Raman band at 820 cm^{-1}. Possible assignments for 820 and 823 cm^{-1} are ν_{20} and $2\nu_{12}$ (816 cm^{-1}). An assignment of 823 cm^{-1} for ν_{20} gives the best numerical fit.

b_{2u} Modes. Proposed assignments: 3068, 1474, 1296, 1174, 999 and 588 cm^{-1}. Of these, all but 3068 and 1174 cm^{-1} are reasonably secure, as they are based on distinct infrared bands that agree well with predicted frequencies. ν_{22} (predicted 3062 cm^{-1}) could possibly be interchanged with the high-frequency $\nu_{13}(b_{1u})$ mode, as discussed above, and ν_{25} (predicted 1176 cm^{-1}) could be interchanged with $\nu_{16}(b_{1u})$ (predicted 1162 cm^{-1}).

b_{3g} Modes. Proposed assignments: 3067, 1540, 1274, 954 and 549 cm^{-1}. Of these assignments, 1540 and 954 cm^{-1} are reasonably secure, being based on distinct Raman bands that agree well with predicted frequencies. The 1274 cm^{-1} assignment is based on intensity, frequency and polarization ratios for this band and the neighboring polarized bands. ν_{33} (predicted 542 cm^{-1}) has been assigned to the Raman band at 549 cm^{-1}, as discussed above. No experimental assignment can be proposed for ν_{30} (predicted 1449 cm^{-1}).

b_{3u} Modes. Proposed assignments: 907, 508 and 215 cm^{-1}. All three modes correlate with distinct infrared bands, but problems with the 907 cm^{-1} assignment have been mentioned above.

It is clear that the density and anharmonicity of vibrational modes for 1458-TAN are such that Fermi resonance (anharmonic coupling) has a marked effect on the observed spectrum. The solution Raman spectrum, although relatively weak, exposes some of these resonances by inducing solvent shifts. Some of the resonant combinations or overtones have not been conclusively identified, and we cannot rule out the possibility that some low-frequency modes, perhaps including the a_u modes, are sufficiently anharmonic that their overtone or combination frequencies cannot be accurately predicted within the harmonic approximation. As shown below, pteridine also shows a number of Fermi resonances, and this is facilitated by the lower number of irreducible representations for the C_s point group—there are many more possible a′ overtones or combinations than there are a_g overtones or combinations for 1458-TAN.

This study has led to a substantial revision of the assignments by Palmer,[13] most of which had been adopted by Carrano and Wait.[10] There is, however, good agreement with all but one (ν_{32}) of the assignments by Chappell and Ross,[17] who assigned 13 modes below 1000 cm^{-1}. This shows that, despite these authors' misgivings, their transferable force field can work well for highly

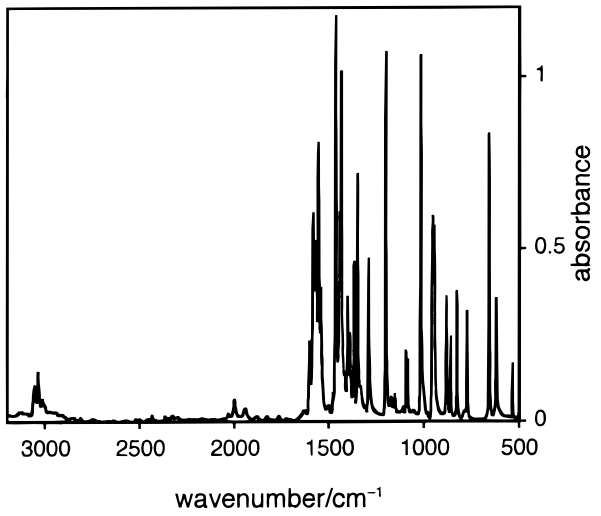

Figure 4. Infrared absorption spectrum of pteridine.

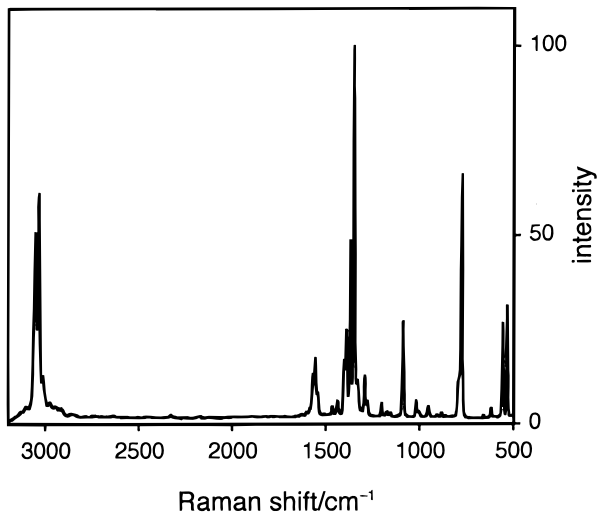

Figure 5. Raman spectrum of pteridine.

aza-substituted naphthalenes. However, some assignments, especially those of the a_u modes, are not yet secure.

Pteridine. The infrared and solid-state Raman spectra of pteridine are shown in Figures 4 and 5, respectively. In Table 5, the computed HF and B3LYP frequencies are compared with the experimental frequencies as well as the assignments of Chappell and Ross.[17] Details of the band assignments are given in Tables 6 and 7. Many sections of these spectra were easy to assign, but others were comparatively difficult. Nineteen modes (eight a′ and 11 a″) are predicted to occur below 1050 cm^{-1}; since all of these are both infrared and Raman active they cannot be separated on the basis of symmetry selection rules, although depolarization ratios were often useful for assigning the stronger bands. Above 1050 cm^{-1}, most bands and all fundamentals were of a′ symmetry and were polarized in the Raman spectrum. The number of spectroscopically active fundamentals, overtones and combinations is high enough for Fermi resonances to be fairly common for this relatively low-symmetry molecule, and this further complicates the analysis. Several such resonances are proposed in our band assignments, and indeed some sections of the spectrum are quite tangled. However, once a satisfactory set of low-frequency fundamentals had been settled on, analysis of most of the higher-frequency bands was fairly straightforward. Differences between theory and experiment are shown in Table 2. The lower symmetry of this compound implies considerably greater computational effort for an MP2 calculation than for 1458-TAN. Given the relatively poor performance of MP2 for the latter, an analogous calculation for pteridine was felt not to be worthwhile.

TABLE 5: Calculated and Experimental Vibrational Frequencies for Pteridine

	$\bar{\nu}/cm^{-1}$				
mode	HF/6-31G*	B3LYP/6-31G*	B3LYP/4-31G	expt[a]	expt[b]
a′ modes					
ν_1	3040	3075	3108	3055	
ν_2	3026	3066	3083	∼3050	
ν_3	3021	3057	3075	3036	
ν_4	3008	3047	3064	3014	
ν_5	1638	1580	1540	∼1570	
ν_6	1628	1560	1525	1557	
ν_7	1602	1532	1486	1543	
ν_8	1486	1451	1430	1465	
ν_9	1449	1432	1409	1440	
ν_{10}	1393	1388	1380	1395	
ν_{11}	1356	1360	1349	1368	
ν_{12}	1333	1332	1320	1350	
ν_{13}	1299	1286	1277	1292	
ν_{14}	1281	1271	1260	1279	
ν_{15}	1198	1186	1163	1202	
ν_{16}	1131	1169	1151	1154	
ν_{17}	1064	1083	1058	1091	
ν_{18}	957	1012	1020	1017	
ν_{19}	938	928	921	954	952
ν_{20}	842	845	843	882	860
ν_{21}	765	759	751	775	773
ν_{22}	599	605	611	620	616
ν_{23}	545	543	550	557	
ν_{24}	516	518	524	535	530
ν_{25}	408	411	413	423	421
a″ modes					
ν_{26}	1022	974	993	1005	980
ν_{27}	1002	960	983	∼950	
ν_{28}	962	920	938	948	945
ν_{29}	884	851	876	860	882
ν_{30}	826	812	846	827	828
ν_{31}	655	654	671	658	658
ν_{32}	514	496	519	498	497
ν_{33}	466	449	466	450	449
ν_{34}	410	389	403	392	391
ν_{35}	187	183	189	204	
ν_{36}	173	154	158	165	

[a] This work. [b] Reference 17.

Most of the bands in the spectra were easily assigned: there was generally good agreement between predicted and observed frequencies, and band polarizations and qualitative intensities were generally consistent with these assignments. After the spectra had been assigned on these grounds, the trends in infrared band intensities were compared with the B3LYP/6-31G* predictions. Pteridine serves as a good test compound, since all its modes are infrared active. As for 1458-TAN, there was reasonably good correlation between theory and experiment, except for some of the highest-frequency modes, notably the C−H stretching modes $\nu_1-\nu_4$. This correlation was examined after the spectra had been assigned using other criteria and was subsequently used to revise some debatable assignments in the 850−1000 cm^{-1} region. These assignments are discussed below, together with others for which band polarizations are ambiguous or unobtainable, and where the possibility or probability of Fermi resonance has been used to explain the proliferation of bands.

On frequency and intensity grounds the bands at 392 cm^{-1} (Raman: fairly strong, slightly polarized; IR: not seen) and 423 cm^{-1} (Raman: weak and polarized; IR: strong) could be assigned to ν_{34} (a″; predicted 389 cm^{-1}) and ν_{25} (a′; predicted 411 cm^{-1}), but the band polarizations suggest that these assignments should be exchanged. The apparent participation

TABLE 6: Band Assignments for the Infrared Spectrum of Pteridine

$\bar{\nu}$/ cm^{-1}	rel intens	pred intens[a]	assignment	$\bar{\nu}$(assigned)/ cm^{-1}	$\Delta\bar{\nu}$[b]/ cm^{-1}
423	41	3.17	ν_{25}(a′)	423	
450	62	15.11	ν_{33}(a″)	450	
498	13	2.19	ν_{32}(a″)	498	
535	13	0.58	ν_{24}(a′)	535	
620	30	9.73	ν_{22}(a′)	620	
658	71	11.49	ν_{31}(a″)	658	
775	27	5.85	ν_{21}(a′)	775	
786	1.9		$2\nu_{34}$(a″)	2 × 392	2
827	32	2.61	ν_{30}(a″)	827	
860	20	9.41	ν_{29}(a″)	860	
882	29	7.30	ν_{20}(a′)	882	
947	49	11.33	ν_{28}(a″)...$\nu_{23}+\nu_{34}$	948	−1
∼950	sh		ν_{28}(a″)...$\nu_{23}+\nu_{34}$		
		0.13	ν_{27}(a″)?	∼950	
954	51	27.33	ν_{19}(a′)	954	
1017	91	21.53	ν_{18}(a′)	1017	
1086	13	7.04	ν_{17}(a′)...($\nu_{23}+\nu_{24}$)	1091	−5
1094	15		ν_{17}...($\nu_{23}+\nu_{24}$)	557 + 535	2
1107	1.4				
1154	4	1.77	ν_{16}(a′)	1154	
1173	2.7		ν_{22}(a′) + ν_{23}(a′)	620 + 557	−4
1202	92	16.75	ν_{15}(a′)	1202	
1288	sh		ν_{29}(a″) + ν_{25}(a′)	860 + 423	5
1292	39	3.92	ν_{13}(a′)	1292	
1306	1.0		ν_{20}(a′) + ν_{25}(a′)	882 + 423	1
1332	1.5				
1350	60	6.47	ν_{12}(a′)	1350	
1368	38	6.78	ν_{11}(a′)	1368	
1389	20	3.59	ν_{10}(a′)...($\nu_{21}+\nu_{22}$)	1395	−6
1402	29		ν_{10}(a′)...($\nu_{21}+\nu_{22}$)	775 + 620	7
1418	2.4				
1436	86	50.24	ν_{9}(a′)...($\nu_{18}+\nu_{25}$)	1440	−4
1443	51		ν_{9}(a′)...($\nu_{18}+\nu_{25}$)	1017 + 423	3
1465	100	35.11	ν_{8}(a′)	1465	
1477	2		ν_{17}(a′) + ν_{34}(a″)	1091 + 392	−6
			ν_{22}(a′) + ν_{29}(a″)	620 + 860	−3
1500	1.3		ν_{20}(a′) + ν_{22}(a′)	882 + 620	−2
1543	31	45.81	ν_{7}(a′)	1543	
∼1550	sh		$2\nu_{21}$(a′)	2 × 775	0
1557	68	19.12	ν_{6}(a′)	1557	
1570	43	69.94	ν_{5}(a′)...$\nu_{16}+\nu_{25}$	1570	0
1577	40		ν_{5}(a′)...$\nu_{16}+\nu_{25}$	1154 + 423	0
			ν_{5}(a′)...$\nu_{18}+\nu_{23}$	1017 + 557	3
1584	50		Fermi?		
1602	18		ν_{30}(a″) + ν_{21}(a′)	827 + 775	0
1620	1.0		ν_{22}(a′) + ν_{26}(a″)	620 + 1005	−5
1635	1.3		ν_{18}(a′) + ν_{22}(a′)	1017 + 620	−2
1763	1.0		ν_{15}(a′) + ν_{23}(a′)	1202 + 557	4
1826	0.9		ν_{13}(a′) + ν_{24}(a′)	1292 + 535	−1
			ν_{15}(a′) + ν_{22}(a′)	1202 + 620	4
1878	0.9		ν_{18}(a′) + ν_{29}(a″)	1017 + 860	1
1942	2.8		ν_{9}(a′) + ν_{32}(a″)	1440 + 498	4
1999	5		ν_{8}(a′) + ν_{24}(a′)	1465 + 535	−1
2030	1.5		$2\nu_{18}$(a′)	2 × 1017	−4
2951	0.3		ν_{6}(a′) + ν_{10}(a′)	1557 + 1395	−1
3003	sh		ν_{7}(a′) + ν_{8}(a′)	1543 + 1465	−5
			ν_{6}(a′) + ν_{9}(a′)	1557 + 1440	6
3014	4	8.90	ν_{4}(a′)	3014	
3036	11	11.38	ν_{3}(a′)	3036	
3055	8	35.69, 22.59	ν_{1}(a′) and ν_{2}(a′)	3055	
3097	0.6				
3126	0.9		ν_{5}(a′) + ν_{6}(a′)	∼1570 + 1557	−1

[a] B3LYP/6-31G* predictions (this work) in units of km mol^{-1}. [b] $\Delta\bar{\nu}$ = $\bar{\nu}$(infrared) − $\bar{\nu}$(assigned).

TABLE 7: Band Assignments for the Raman Spectrum of Pteridine

$\bar{\nu}$/ cm^{-1}	pol/depol[b]	rel intens	assignment	$\bar{\nu}$(assigned)/ cm^{-1}	$\Delta\bar{\nu}$[a]/ cm^{-1}
165	d	3.6	ν_{36}(a″)	165	
204	d	3.0	ν_{35}(a″)	204	
392	sl. p	10.7	ν_{34}(a″)	392	
424	p	1.4	ν_{25}(a′)	423	1
450	−	1.2	ν_{33}(a″)	450	
499	−	1.0	ν_{32}(a″)	498	1
534	p	29.6	ν_{24}(a′)	535	−1
557	p	25.5	ν_{23}(a′)	557	
619	sl p	2.4	ν_{22}(a′)	620	−1
659	−	0.6	ν_{31}(a″)	658	1
776	p	65.4	ν_{21}(a′)	775	1
786	p	12.0	$2\nu_{34}$(a″)	2 × 392	2
828	−	0.6	ν_{30}(a″)	827	1
861	−	0.6	ν_{29}(a″)	860	1
882	p	1.4	ν_{20}(a′)	882	
907	p	0.8			
953	sl p	3.0	ν_{19}(a′)	954	−1
1005	−	1.6	ν_{26}(a″)	1005	
1018	p	4.6	ν_{18}(a′)	1017	1
1087	p	25.7	ν_{17}(a′)...($\nu_{23}+\nu_{24}$)	1091	−4
1154	p	1.1	ν_{16}(a′)	1154	
1174	p	1.5	ν_{22}(a′) + ν_{23}(a′)	620 + 557	−3
1202	p	3.9	ν_{15}(a′)	1202	
1279	p	4.4	ν_{14}(a′)	1279	
1292	p	11.2	ν_{13}(a′)	1292	
1305	p	2.4	ν_{20}(a′) + ν_{25}(a′)	882 + 423	0
			ν_{21}(a′) + ν_{24}(a′)	775 + 535	−5
1329	p	10.0	ν_{21}(a′) + ν_{23}(a′)	775 + 557	−3
1350	p	100	ν_{12}(a′)	1350	
1369	p	47.7	ν_{11}(a′)	1368	
1390	p	23.7	ν_{10}(a′)...($\nu_{21}+\nu_{22}$)	1395	−5
1403	p	15.4	ν_{10}(a′)...($\nu_{21}+\nu_{22}$)	775 + 620	8
1437	p	4.3	ν_{9}(a′)...($\nu_{18}+\nu_{25}$)	1440	−3
1465	p	2.8	ν_{8}(a′)	1465	
1543	p	6.4	ν_{7}(a′)	1543	
1556	p	16.0	ν_{6}(a′)	1557	−1
1571	p	11.6	ν_{5}(a′) Fermi?	∼1570	
1588	p	2.4	Fermi?		
1602	−	1.5	ν_{30}(a″) + ν_{21}(a′)	827 + 775	0
2329	−	0.6	ν_{6}(a′) + ν_{21}(a′)	1557 + 775	−3
2920	−	3.0	ν_{6}(a′) + ν_{11}(a′)	1557 + 1368	−5
2947	−	3.0	ν_{6}(a′) + ν_{10}(a′)	1557 + 1395	−5
2976	−	4.4			
3014	p	11.7	ν_{4}(a′)	3014	
3027	−		ν_{6}(a′) + ν_{8}(a′)	1557 + 1465	5
3036	p	60.6	ν_{3}(a′)	3036	
3056	p	50.3	ν_{1}(a′) and ν_{2}(a′)	3055	
3105	p	3.4	$2\nu_{6}$(a′)	2 × 1557	−9

[a] $\Delta\bar{\nu}$ = $\bar{\nu}$(Raman) − $\bar{\nu}$(assigned). [b] Polarization measurements obtained in saturated chloroform solution. − denotes that a band was not seen, or obscured by solvent bands.

of these intervals in combination bands (see Tables 6 and 7) supports the former assignment. The bands between 425 and 600 cm^{-1} present no problems, but it is hard to find a convincing assignment for ν_{22} (a′; predicted 605 cm^{-1}) in this rather sparse spectral region. We have settled on the weak, slightly polarized Raman band at 619 cm^{-1}, as the stronger polarized Raman bands at 534, 557 and 776 cm^{-1} may be assigned to ν_{24} (a′; predicted 518 cm^{-1}), ν_{23} (a′; predicted 543 cm^{-1}) and ν_{21} (a′; predicted 759 cm^{-1}; note the possible Fermi resonance with $2\nu_{34}$), respectively, and the strong infrared band at 658 cm^{-1} is assigned to ν_{31} (a″; predicted 654 cm^{-1}).

The next assignments that require comment are in the 850−1000 cm^{-1} region, where there do not appear to be enough bands to accommodate all the predicted fundamentals. The B3LYP/6-31G* infrared intensities have helped to evaluate the range of possible assignments. The assignment of the moderately strong infrared band at 882 cm^{-1} (polarized in the Raman spectrum) to ν_{20} (a′; predicted 845 cm^{-1}) is fairly secure despite the relatively large difference between the calculated and experimental frequencies (37 cm^{-1}). The moderately strong infrared band at 860 cm^{-1} also correlates well on intensity and frequency grounds with ν_{29} (a″; predicted 851 cm^{-1}). The weak Raman band (not seen in the infrared) at 1005 cm^{-1} is assigned

to ν_{26} (a″; predicted 974 cm^{-1}) despite the relatively large frequency difference (31 cm^{-1}). This leaves three modes to be assigned: ν_{28} (a″; predicted 920 cm^{-1}; predicted to be strong in the infrared spectrum), ν_{19} (a′; predicted 928 cm^{-1}; strong infrared) and ν_{27} (a″; predicted 960 cm^{-1}; weak infrared). The unassigned bands in this region are a very weak, polarized Raman band at 907 cm^{-1} (not seen in the infrared spectrum) and a cluster of bands at about 950 cm^{-1} in the infrared spectrum; there is a single, slightly polarized Raman band at 953 cm^{-1}. We cannot find a convincing assignment for the 907 cm^{-1} band, which is in any case very weak. The higher-frequency component of the broad composite band near 950 cm^{-1} is assigned to ν_{19}; there is a corresponding band in the Raman spectrum. On infrared intensity grounds the lower-frequency component is attributable to ν_{28}, possibly in resonance with $\nu_{23} + \nu_{34}$ (a″; calculated 949 cm^{-1}); ν_{27} may also make a small contribution to the overall band.

Although it is hard to find enough bands to accommodate all the predicted fundamentals in the 850−1000 cm^{-1} region, the opposite is true above 1000 cm^{-1}. The strong infrared and Raman bands at about 1017 cm^{-1} are almost certainly attributable to ν_{18} (a′; predicted 1012 cm^{-1}). The next major feature in the spectrum is the strong polarized band at 1087 cm^{-1} in the pure crystal Raman spectrum, which corresponds to a 1086/1094 cm^{-1} doublet in the infrared spectrum. The solution Raman spectrum also appears to contain a doublet, which we attribute to a Fermi resonance between the ν_{17} fundamental (a′; predicted 1083 cm^{-1}) and the $\nu_{23} + \nu_{24}$ combination (a′; 1091 cm^{-1}). ν_{17} would therefore have an unperturbed frequency of about 1091 cm^{-1}. The Raman spectrum contains weak, polarized bands at 1154 and 1174 cm^{-1}, which we assign to ν_{16} (a′; predicted 1169 cm^{-1}) and the $\nu_{22} + \nu_{23}$ combination (a′; 1177 cm^{-1}). ν_{15} (a′; predicted 1186 cm^{-1}) could be assigned either to the weak band at 1174 cm^{-1} or the stronger polarized band at 1202 cm^{-1}; we prefer 1202 cm^{-1}.

The 1250−1500 cm^{-1} region contains eight prominent infrared bands, ten Raman bands (three of which do not have infrared counterparts) and seven predicted a′ fundamentals: ν_8−ν_{14}, with predicted frequencies of 1271, 1286, 1332, 1360, 1388, 1432 and 1451 cm^{-1}. All solution-phase Raman bands are polarized. The proliferation of closely spaced bands, for example the doublets at 1389/1402 and 1436/1443 cm^{-1}, suggests that one or more Fermi resonances may be occurring in this region. The pair of solid-state Raman bands at 1279 and 1292 cm^{-1} change their relative intensities in the solution spectrum, suggesting that they may possibly be a Fermi doublet, and the strength of coupling is solvent-dependent. The single strong band at 1369 cm^{-1} in the solid-state spectrum turns into a 1368/1378 cm^{-1} doublet in solution, indicating the ease with which Fermi resonance occurs in this compound.

The strong infrared band at 1465 cm^{-1} (polarized in the Raman spectrum) is presumably ν_8 (a′; predicted 1451 cm^{-1}). The 1436/1443 cm^{-1} infrared doublet (seen as a 1437 cm^{-1} singlet in the Raman spectrum) is assigned to ν_9 (a′; predicted 1432 cm^{-1}), in resonance with $\nu_{18} + \nu_{25}$ (a′; 1440 cm^{-1}). Thus, ν_9 would have an unperturbed frequency of about 1440 cm^{-1}. Owing to their high intensities in the corresponding Raman spectrum, the infrared bands at 1350, 1368 and 1389/1402 cm^{-1} (doublet) are assigned to ν_{12} (predicted 1332 cm^{-1}), ν_{11} (predicted 1360 cm^{-1}) and ν_{10} (predicted 1388 cm^{-1}). The band at 1403 cm^{-1} is attributed to Fermi resonance between ν_{10} and $\nu_{21} + \nu_{22}$ (a′; 1395 cm^{-1}), suggesting an unperturbed frequency of about 1395 cm^{-1} for ν_{10}. This leaves ν_{13} (predicted 1286 cm^{-1}) and ν_{14} (predicted 1271 cm^{-1}) to be assigned in this region of the spectrum. We propose that these fundamentals should be assigned to the strongest and otherwise unassigned Raman bands: 1292 and 1279 cm^{-1}, respectively. The 1292 cm^{-1} band and its shoulder at 1288 cm^{-1} in the infrared spectrum show some matrix dependence, but in the absence of a convincing a′ combination or overtone we suggest that 1288 cm^{-1} might possibly be attributable to $\nu_{29} + \nu_{25}$ (a″; 1293 cm^{-1}). The weak polarized Raman bands at 1305 and 1329 cm^{-1} are assigned to $\nu_{20} + \nu_{25}$ (a′; 1305 cm^{-1}) and/or $\nu_{21} + \nu_{24}$ (a′; 1310 cm^{-1}), and $\nu_{21} + \nu_{23}$ (a′; 1332 cm^{-1}), respectively.

The 1500−1650 cm^{-1} region contains six prominent infrared bands (with traces of other, weaker bands), five Raman bands (which correlate reasonably well with the infrared spectrum) and three predicted a′ fundamentals, ν_5−ν_7, with predicted frequencies of 1532, 1560 and 1580 cm^{-1}. Again, it seems likely that one or more Fermi resonances are implicated, but unfortunately the solution-phase Raman spectrum is too weak to be of significant help to evaluate this possibility. On frequency and intensity grounds we assign the strong bands at 1557 and 1543 cm^{-1}, seen in both spectra, to ν_6 (a′; predicted 1560 cm^{-1}) and ν_7 (a′; predicted 1532 cm^{-1}), respectively. ν_5 (a′; predicted 1580 cm^{-1}) may be associated with one or more of the prominent bands at 1570 cm^{-1} (infrared and Raman), 1584 cm^{-1} (infrared only) and 1588 cm^{-1} (Raman only). Resonances with $\nu_{16} + \nu_{25}$ (a′; 1577 cm^{-1}) and $\nu_{18} + \nu_{23}$ (a′; 1574 cm^{-1}) are possible, and the appearance of the spectra suggests that the interaction may be quite complex.

In the C−H stretching region there are strong Raman bands at 3036 and 3056 cm^{-1}, and weaker features at 3027 and 3014 cm^{-1}. The spectrum is polarized, with a different distribution of band intensities in solution. The infrared spectrum contains strong bands at 3014, 3036 and 3055 cm^{-1}, and a shoulder at 3003 cm^{-1}. In both spectra the band at 3055 cm^{-1} is relatively broad and could be composite. The ν_1-ν_4 modes are predicted to occur at 3075, 3066, 3057 and 3047 cm^{-1}, respectively. Three of these fundamentals may be assigned to the 3055, 3036 and 3014 cm^{-1} bands, but the assignment of a particular band to one or other of these modes is rather arbitrary, owing to the relatively close spacing of the predicted frequencies. The fourth fundamental could be assigned to one of the weak infrared or Raman bands below 3000 cm^{-1}, or to one of the shoulders. Alternatively, as the 3055 cm^{-1} band appears to be broadened on the low-frequency side and it is difficult to identify a combination or overtone that might induce an apparent broadening through Fermi resonance, it is possible that a weaker fundamental band occurs at about 3050 cm^{-1}. This point cannot be settled conclusively, so we tentatively suggest that the remaining fundamental lies near 3050 cm^{-1}. The B3LYP/6-31G* infrared intensities appear to be somewhat unreliable in this frequency range.

This study is the first comprehensive analysis of the vibrational spectra of pteridine, especially for the higher-frequency modes. For all but three modes (ν_{20}, ν_{26} and ν_{29}) our results agree with those of Chappell and Ross,[17] who assigned 14 of the modes below 1000 cm^{-1}.

2367-TAN. The available sample of 2367-TAN was too small to permit further purification, and only one infrared absorption spectrum could be recorded (Figure 6). However, the bands in this spectrum matched the only reported vibrational frequencies,[14] indicating that the material was substantially pure. Although experimental data for this compound are sparse, the good fit between theory and experiment for the vibrational frequencies that are available, and the encouraging results for

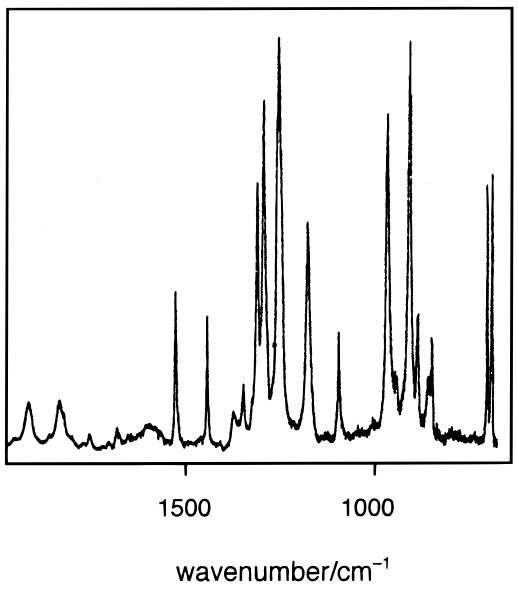

Figure 6. Infrared absorption spectrum of 2367-TAN.

1458-TAN and pteridine, indicate that the predicted but unseen frequencies are likely to be reasonably accurate.

Table 8 lists the experimental and calculated vibrational frequencies for 2367-TAN, together with our assignments for 12 of the fifteen infrared-active modes. Since there was not enough compound to allow a Raman spectrum to be recorded, no experimental data are available for the a_g, b_{1g}, b_{2g} and b_{3g} modes. As with the other two compounds, the DFT frequencies for the infrared-active fundamentals correlate well with the observed spectrum, and most of the other bands in the spectrum may be provisionally assigned to combinations of these fundamentals and predicted frequencies. Table 9 contains our proposed assignments for the spectrum shown in Figure 6. Our assignments for the combination bands were chosen to give reasonable numerical fits, but since they all rely on at least one calculated frequency, they indicate what is possible and reasonable, rather than conclusive. Differences between theory and the limited number of experimentally assigned fundamentals are shown in Table 2.

A few assignments deserve particular comment. There are two strong bands at 676 and 688 cm^{-1} in the infrared spectrum, either of which could be assigned to ν_{27} (b_{2u}; predicted 675 cm^{-1}). We have chosen the assignment that gives the best numerical fit, but the alternative 688 cm^{-1} assignment is also plausible. This would require the 676 cm^{-1} band to be reassigned as $\nu_{33} + \nu_{10}$, and 1929 cm^{-1} as, for example, $\nu_{34} + \nu_5$. We have explored the possibility of a Fermi resonance that might explain the similar intensities of the fundamental and combination bands, but no b_{2u} combinations lie nearby.

For intensity reasons, the strong band at 959 cm^{-1} has been assigned to the ν_{34} mode of b_{3u} symmetry although an assignment to the weaker band at 929 cm^{-1} would give a better fit with the predicted frequency of 921 cm^{-1}. A 929 cm^{-1} assignment would make it difficult to assign the 1369 cm^{-1} combination band satisfactorily. Again, we have considered the possibility of a Fermi resonance, but have found no suitable b_{3u} combination to interact with ν_{34}. Finally, the bands at 1288 and 1306 cm^{-1} have been assigned to ν_{24} and ν_{15}, respectively, on the basis of their predicted frequencies (1282 and 1290 cm^{-1}, respectively) but a rearrangement of the assignments would be possible.

Comparisons with Naphthalene. As mentioned in the Introduction, there are marked similarities between the vibrational spectra of naphthalene and the monoaza- and diazanaphthalenes; Carrano and Wait[10] have published a table that compares the vibrational frequencies for naphthalene and various azanaphthalenes, including 1458-TAN. We have extended and revised this work by correlating the normal modes of naphthalene with those of 1458-TAN, 2367-TAN and pteridine using the results of our HF/6-31G* calculations and Lane's WINVIB program.[29] The correlations are summarized in Table 10, and a more extensive table for all the tetraazanaphthalenes is reported elsewhere.[7] Strictly speaking, Table 10 correlates the modes of 1458-TAN with those of naphthalene, and the other two tetraazanaphthalenes with 1458-TAN. A detailed comparison of the normal modes is outside the scope of the present paper, but overall there is a clear correlation between the modes of 1458-TAN and naphthalene, once allowance has been made for the larger number of modes in naphthalene, as required by the larger number of possible C−H stretching and bending motions. In many cases there is a one-to-one correspondence of modes, although there are some exceptions: for example the 1389 cm^{-1} mode for 1458-TAN resembles both modes ν_{20} and ν_5 for naphthalene. There are also clear correlations between the modes

TABLE 8: Calculated and Experimental Vibrational Frequencies for 2367-TAN

	$\bar{\nu}$/cm^{-1}				
mode	HF/6-31G*	B3LYP/6-31G*	B3LYP/4-31G	IR[a]	IR[b]
a_g modes					
ν_1	3024	3064	3074		
ν_2	1624	1563	1542		
ν_3	1423	1401	1380		
ν_4	1329	1296	1274		
ν_5	1008	964	860		
ν_6	810	811	805		
ν_7	494	500	503		
a_u modes					
ν_8	951	921	937		
ν_9	678	663	666		
ν_{10}	175	162	164		
b_{1g} modes					
ν_{11}	894	855	878		
ν_{12}	389	344	349		
b_{1u} modes					
ν_{13}	3022	3061	3072		3065
ν_{14}	1593	1521	1479	1535	1530
ν_{15}	1305	1290	1297	1306	1308
ν_{16}	1223	1235	1235	1253	1250
ν_{17}	798	805	797	835	
ν_{18}	333	329	337		
b_{2g} modes					
ν_{19}	971	941	966		
ν_{20}	790	782	792		
ν_{21}	448	401	408		
b_{2u} modes					
ν_{22}	3019	3060	3072		3020
ν_{23}	1446	1434	1413	1447	1445
ν_{24}	1331	1283	1263	1288	1290
ν_{25}	1132	1161	1159	1171	1170
ν_{26}	913	916	803	894	892
ν_{27}	673	675	679	676	680
b_{3g} modes					
ν_{28}	3019	3059	3070		
ν_{29}	1659	1592	1566		
ν_{30}	1355	1315	1282		
ν_{31}	1256	1257	1266		
ν_{32}	950	948	946		
ν_{33}	514	514	525		
b_{3u} modes					
ν_{34}	956	921	952	959	953
ν_{35}	491	467	474		478
ν_{36}	168	160	164		

[a] This work. [b] Reference 11.

TABLE 9: Band Assignments for the Infrared Spectrum of 2367-TAN

$\bar{\nu}$(infrared)/ cm^{-1}	rel intens	assignment	ν(assigned)/ cm^{-1}	$\Delta\bar{\nu}^a$/ cm^{-1}
478[b]		$\nu_{35}(b_{3u})$	478	
676	69	$\nu_{27}(b_{2u})$	676	
688	66	$\nu_{33}(b_{3g}) + \nu_{10}(a_u)$	514[c] + 162[c]	12
835	32	$\nu_{17}(b_{1u})$	835	
847	23	$\nu_{33}(b_{3g}) + \nu_{18}(b_{1u})$	514[c] + 329[c]	4
873	37	$\nu_{35}(b_{3u}) + \nu_{21}(b_{2g})$	478 + 401[c]	−6
894	100	$\nu_{26}(b_{2u})$	894	
929	32	$\nu_{20}(b_{2g}) + \nu_{36}(b_{3u})$	782[c] + 160[c]	−13
		$\nu_{20}(b_{2g}) + \nu_{10}(a_u)$	782[c] + 162[c]	−15
959	83	$\nu_{34}(b_{3u})$	959	
1088	37	$\nu_{19}(b_{2g}) + \nu_{36}(b_{3u})$	941[c] + 160[c]	−13
		$\nu_{19}(b_{2g}) + \nu_{10}(a_u)$	941[c] + 162[c]	−15
1171	54	$\nu_{25}(b_{2u})$	1171	
1253	100	$\nu_{16}(b_{1u})$	1253	
1288	88	$\nu_{24}(b_{2u})$	1288	
1306	67	$\nu_{15}(b_{1u})$	1306	
1347	21	$\nu_{17}(b_{1u}) + \nu_{33}(b_{3g})$	835 + 514[c]	−2
1369	15	$\nu_{34}(b_{3u}) + \nu_{21}(b_{2g})$	959 + 401[c]	9
1411	8	$\nu_{26}(b_{2u}) + \nu_{33}(b_{3g})$	894 + 514[c]	3
1447	36	$\nu_{23}(b_{2u})$	1447	
1535	42	$\nu_{14}(b_{1u})$	1535	
1688	11	$\nu_{25}(b_{2u}) + \nu_{33}(b_{3g})$	1171 + 514[c]	3
1764	9	$\nu_{16}(b_{1u}) + \nu_{33}(b_{3g})$	1253 + 514[c]	−3
1847	17	$\nu_{32}(b_{3g}) + \nu_{26}(b_{2u})$	948[c] + 894	5
1871	9	$\nu_{32}(b_{3g}) + \nu_8(a_u)$	948[c] + 921[c]	2
1929	16	$\nu_{31}(b_{3g}) + \nu_{27}(b_{2u})$	1257[c] + 676	−4
1967	8	$\nu_{23}(b_{2u}) + \nu_{33}(b_{3g})$	1447 + 514[c]	6
		$\nu_4(a_g) + \nu_{27}(b_{2u})$	1296[c] + 676	−5
3020[b]		$\nu_{22}(b_{2u})$		
3065[b]		$\nu_{13}(b_{1u})$		

[a] $\Delta\bar{\nu} = \bar{\nu}$(infrared) − $\bar{\nu}$(assigned). [b] Data from ref 14. [c] Scaled B3LYP/6-31G* frequencies.

of the two D_{2h} tetraazanaphthalenes, 1458-TAN and 2367-TAN, but correlations become harder to discern for many of the less-symmetric C_s molecules. Nevertheless it is possible to correlate the modes of 1458-TAN and pteridine, as shown in Table 10, and there is reasonably good numerical agreement between the corresponding modes of the different molecules. This justifies the earlier use of comparisons between vibrational spectra of related azanaphthalenes as a tool for spectral assignment, but improved spectra and the use of ab initio and density-functional calculations have altered a substantial number of the earlier assignments and correlations by Palmer[13] and Carrano and Wait.[10]

IV. Conclusions

New vibrational spectra have been recorded and analyzed for 1458-TAN and pteridine, and a more limited study is reported for 2367-TAN. It was found that scaled B3LYP/6-31G* frequencies give the best agreement with experiment and allow most of the ground-state normal modes to be assigned for these compounds. Therefore, reasonably accurate predictions are now available for frequencies that have not yet been measured experimentally. The correlation between calculated gas-phase infrared intensities and the solid-state infrared spectra is good enough for these to be useful in assigning the spectra, except in the C−H stretching region near 3000 cm^{-1}.

Although scaled B3LYP/4-31G calculations give the best fit to the vibrational spectra of naphthalene, they perform less well for the three tetraazanaphthalenes that we have studied. Nevertheless, the computationally more economical 4-31G basis should still give reasonably accurate results for larger aza-substituted molecules, particularly when the number of nitrogen atoms is small. This will be important for compounds such as 1,10-phenanthroline, which has 31 normal modes in the range 400−1200 cm^{-1}, compared with 20 for 1458-TAN.[23] Larger molecules will have even greater densities of modes.

A notable feature of these tetraazanaphthalene spectra is the proliferation of Fermi resonances, even for the D_{2h} molecule, 1458-TAN. These molecules appear to be much more suscep-

TABLE 10: Correlation of Vibrational Frequencies and Symmetries for Naphthalene, 1458-TAN, 2367-TAN and Pteridine

naphthalene mode	$\bar{\nu}$/cm^{-1}			
	naphthalene[a]	1458-TAN[b]	2367-TAN[d]	pteridine[b]
a_g modes				
ν_1	3057.2	3052[c]	3064*	3055 (a′)
ν_2	3004			
ν_3	1576.4	1563	1563*	1543 (a′)
ν_4	1464.4	1375	1401*	1395 (a′)
ν_5	1380	1342	1296*	1350 (a′)
ν_6	1146?			
ν_7	1020	1054	964*	1091 (a′)
ν_8	761	763	811*	775 (a′)
ν_9	516	552	500*	535 (a′)
a_u modes				
ν_{10}	982		921*	∼950 (a″)
ν_{11}	844.5	652[c]	663*	658 (a″)
ν_{12}	609*			
ν_{13}	195	121[c]	162*	165 (a″)
b_{1g} modes				
ν_{14}	950	868	855*	860 (a″)
ν_{15}	726.0			
ν_{16}	385	408	344*	392 (a″)
b_{1u} modes				
ν_{17}	3063.6	3052	3061	3036 (a′)
ν_{18}	3054?			
ν_{19}	1601.6	1579	1535	1557 (a′)
ν_{20}	1392.2	1389[e]	1306	1368 (a′)
ν_{21}	1267.6			
ν_{22}	1130	1185[c]	1253	1202 (a′)
ν_{23}	777*	882	835	882 (a′)
ν_{24}	359.3	460	329	423 (a′)
b_{2g} modes				
ν_{25}	982.8	990	941*	1005 (a″)
ν_{26}	878	823	782*	827 (a″)
ν_{27}	773			
ν_{28}	465	469	401*	450 (a″)
b_{2u} modes				
ν_{29}	3078.5	3068[c]	3060*	∼3050 (a′)
ν_{30}	3042			
ν_{31}	1514.2	1474	1447	1465 (a′)
ν_{32}	1361.1	1296	1288	1292 (a′)
ν_{33}	1210.4			
ν_{34}	1134.7	1174[c]	1171	1154 (a′)
ν_{35}	1011.92	999	894	1017 (a′)
ν_{36}	619.5	588	676	620 (a′)
b_{3g} modes				
ν_{37}	3070*	3067	3059*	3014 a′)
ν_{38}	2980			
ν_{39}	1628.7	1540	1592*	∼1571 (a′)
ν_{40}	1445.2		1315*	1440 (a′)
ν_{41}	1243.8	1274	1257*	1279 (a′)
ν_{42}	1168.4			
ν_{43}	939	954	948*	954 (a′)
ν_{44}	509	549	514*	557 (a′)
b_{3u} modes				
ν_{45}	959.00	907	959	948 (a″)
ν_{46}	782.3			
ν_{47}	473.4	508	467*	498 (a″)
ν_{48}	166.2	215	160*	204 (a″)

[a] Experimental frequencies from ref 30, except for the values labeled *, which are scaled B3LYP/6-31G* frequencies. [b] Experimental frequencies from this work. [c] Tentative assignments only. [d] Experimental frequencies from this work, except values labeled *, which are scaled B3LYP/6-31G* predictions. [e] Also resembles naphthalene a_g mode ν_5.

tible to Fermi resonance than the diazanaphthalenes.[10,31] The importance of anharmonic coupling in these molecules, and occasional difficulties in identifying the resonant combinations or overtones, suggest that the harmonic approximation is not particularly satisfactory for some modes. We note, however, that the agreement between the B3LYP/6-31G* and experimental frequencies is, if anything, slightly better for the tetraazanaphthalenes than the parent hydrocarbon, naphthalene.

Acknowledgment. We are grateful to Professor I. G. Ross for a sample of 2367-TAN, Dr W. L. F. Armarego for samples of 1458-TAN and helpful advice on the synthesis and purification of this compound, and Professor A. V. Bree for helpful suggestions about the vibrational analysis.

References and Notes

(1) Innes, K. K.; Byrne, J. P.; Ross, I. G. *J. Mol. Spectrosc.* **1967**, *22*, 125.
(2) Innes, K. K.; Ross, I. G.; Moomaw, W. R. *J. Mol. Spectrosc.* **1988**, *132*, 492.
(3) Fischer, G.; Wormell, P. *Chem. Phys.* **1995**, *198*, 183.
(4) Palmer, M. H.; McNab, H.; Walker, I. C.; Guest, M. F.; MacDonald, M.; Siggel, M. R. F. *Chem. Phys.* **1998**, *228*, 39. Fischer, G.; Smith, D. M.; Nwankwoala, A. U. *Chem. Phys.* **1997**, *221*, 11.
(5) Hurst, J. K.; Wormell, P.; Krausz, E.; Lacey, A. R. *Chem. Phys.* **1999**, *246*, 229.
(6) Pfleiderer, W. In *Unconjugated Pterins in Neurobiology*; Loevenberg, W., Levine, R. A., Eds.; Taylor and Francis: London, 1987.
(7) Hurst, J. K. Ph.D. Thesis, The University of Sydney, 1997.
(8) Hurst, J. K.; Wormell, P.; Reimers, J. R.; Lacey, A. R. *J. Phys. Chem. A* **1999**, *103*, 3089.
(9) Bauschlicher, C. W. *Chem. Phys.* **1998**, *234*, 87.
(10) Carrano, J. T.; Wait, S. C. *J. Mol. Spectrosc.* **1973**, *46*, 401.
(11) Mitchell, R. W.; Glass, R. W.; Merritt, J. A. *J. Mol. Spectrosc.* **1970**, *36*, 310.
(12) Mulliken, R. S. *J. Chem. Phys.* **1955**, *23*, 1997.
(13) Palmer, R. MS Thesis, Rensselaer Polytechnic Institute, 1970.
(14) Adembri, G.; De Sio, F.; Nesi, R.; Scotton, M. *Chem. Commun.* **1967**, 1006.
(15) Mason, S. F. *J. Chem. Soc.* **1955**, 2336.
(16) Armarego, W. L. F.; Barlin, G. B.; Spinner, E. *Spectrochim. Acta* **1966**, *22*, 117.
(17) Chappell, P. J.; Ross, I. G. *J. Mol. Spectrosc.* **1977**, *66*, 192.
(18) Wormell, P.; Lacey, A. R. *Chem. Phys.* **1987**, *118*, 71.
(19) F. Billes, F.; Mikosch, H.; Holly, S. *J. Mol. Struct. (THEOCHEM)* **1998**, *423*, 225.
(20) Bauschlicher, C. W.; Langhoff, S. R. *Spectrochim. Acta* **1997**, *53A*, 1225.
(21) Langhoff, S. R. *J. Phys. Chem.* **1996**, *100*, 2819.
(22) Bauschlicher, C. W.; Langhoff, S. R.; Sandford, S. A. *J. Phys. Chem. A* **1997**, *101*, 2414.
(23) Thornton, D. A.; Watkins, G. M. *Spectrochim. Acta* **1991**, *47A*, 1085.
(24) Albert, A.; Yamamoto, H. *J. Chem. Soc. C* **1968**, 2289.
(25) Armarego, W. L. F. *J. Chem. Soc.* **1963**, 4304.
(26) Frisch, M. J.; Trucks, G. W.; Schlegel, H. B.; Gill, P. M. W.; Johnson, B. G.; Robb, M. A.; Cheeseman, J. R.; Keith, T.; Petersson, G. A.; Montgomery, J. A.; Raghavachari, K.; Al-Laham, M. A.; Zakrzewski, V. G.; Ortiz, J. V.; Foresman, J. B.; Peng, C. Y.; Ayala, P. Y.; Chen, W.; Wong, M. W.; Andres, J. L.; Replogle, E. S.; Gomperts, R.; Martin, R. L.; Fox, D. J.; Binkley, J. S.; Defrees, D. J.; Baker, J.; Stewart, J. P.; Head-Gordon, M.; Gonzalez, C.; Pople, J. A. *Gaussian 94*, Revision B.3; Gaussian Inc.: Pittsburgh, PA, 1995.
(27) Pople, J. A.; Scott, A. P.; Wong, M. W.; Radom, L. *Isr. J. Chem.* **1993**, *33*, 345.
(28) Wong, M. W. *Chem. Phys. Lett.* **1996**, *256*, 391.
(29) *WINVIB program*, S. Lane, Sydney, Australia, 1995.
(30) Canè, E.; Palmieri, P.; Tarroni, R.; Trombetti, A.; Handy, N. C. *Gazz. Chim. Ital.* **1996**, *126*, 289.
(31) Wormell, P.; Bacskay, G. Unpublished results.